Zuerst erschienen in: Nuclear Engineering and Design 234 (2004), Seite 25–43, http://dx.doi.org/10.1016/j.nucengdes.2004.08.002

Plastic collapse analysis of longitudinally flawed pipes and vessels

M. Staat*

Aachen University of Applied Sciences, Div. Jülich, Ginsterweg 1, 52428 Jülich, Germany

Abstract

Improved collapse loads of thick-walled, crack containing pipes and vessels are suggested. Very deep cracks have a residual strength which is better modelled by a global limit load. In all burst tests, the ductility of pressure vessel steels was sufficiently high whereby the burst pressure could be predicted by limit analysis with no need to apply fracture mechanics. The relative prognosis error increases however, for long and deep defects due to uncertainties of geometry and strength data.

1. Introduction

The prediction of the burst pressure of 134 longitudinally flawed pipes and vessels with four engineering methods showed large deviations particularly for deep defects (Stoppler et al., 1992, 1994). The used formulae can be interpreted as local collapse load approximations for thin-walled pipes. The mentioned deviations could not be attributed alone to the statistical uncertainties in geometry and material parameters. Rather, it was assumed that the used plastic collapse load approximations for deep defects are unsuitable. Therefore, 44 deep defects were removed from the assessment in Stoppler et al. (1992, 1994).

This contribution assumes that the materials were sufficiently ductile in all cases, so that plastic collapse has dominated. Therefore, new approximations for collapse loads are suggested, which describe all defect dimensions equally well: long, short, shallow (to defect-free) and deep (including wall penetrating slits). Particularly global collapse loads are proposed, because they can predict the residual strength of very deep cracks and slits. Additionally, all approximations are formulated for thick-walled pipes. The database was extended to 293 burst tests according to this objective and includes now 15 uncracked pipes as well as 30 pipes with penetrating defects.

* Tel.: +49 2461 99 3209; fax: +49 2461 99 3199.
E-mail address: m.staat@fh-aachen.de.

Nomenclature

A_v	Charpy-V notch impact energy
a	crack length
c	crack depth
D	constraint factor
E	Young's modulus
eps	relative prognosis error
F_Y, F_U	yield function, bounding function
f	function
M_FL	Folias factor
M_1, M_2	Folias factor for internal and external defect
$\boldsymbol{n}$	exterior unit normal
$\boldsymbol{P}$	reference load
$\overline{p}_0$, p_0	burst pressure without defect old, new
p_exp, p_formula	experimental, predicted burst pressure
p_global, p_local	global and local collapse pressure
$\overline{p}_\mathrm{L}$, p_L	collapse pressure of defect pipe old, new
p_Y	pressure at first yield
R_1^*, R_1	distinction of crack face loading old, new
r_1, r_2	interior and exterior radius, respectively
R_F	flow stress
$R_{p0.2}$	0.2% strain limit
R_m	ultimate stress
t	wall thickness
V	body
∂V_σ	traction boundary
γ	limit load factor
ν	Poisson's ratio
$\boldsymbol{\rho}$	self-equilibrated stress tensor
$\boldsymbol{\sigma}$	stress tensor
$\boldsymbol{\sigma}^\mathrm{E}$	fictitious elastic stress tensor
σ_y	yield stress
σ_u	ultimate stress
σ_L	collapse stress of plates

The new global collapse load formulae can improve the defect assessment by the two criteria methods (Harrison et al., 1980; R6, 2001) or the engineering treatment method (Schwalbe et al., 1998). In the reference stress approach, the collapse loads can be used to estimate non-linear fracture mechanics parameters such as crack tip opening displacement (CTOD), J and C^* integrals (R5, 2003; R6, 2001).

1.1. Limit load theorems

The local strength of material is measured by the reference stress or by the yield function $F(\boldsymbol{\sigma})$ for instance according to the hypotheses of Tresca or von Mises. Stresses $\boldsymbol{\sigma}$ are admissible in a perfectly plastic material model, if they satisfy the yield condition

$$F(\boldsymbol{\sigma}) \leq \sigma_\mathrm{y}. \tag{1}$$

With equality in one point, the elastic limit (0.2% strain limit) $\sigma_\mathrm{y} = R_{p0.2}$ is assumed and yielding can begin there.

In the context of the two-surface theory of plasticity, the yield surface $F_\mathrm{Y}(\boldsymbol{\sigma}) \leq \sigma_\mathrm{y}$ can harden kinematically within a bounding surface $F_U(\boldsymbol{\sigma}) \leq \sigma_u$. In the simplest theory, the bounding surface is assumed as fixed in size, form and location in stress space. Usually, the same function is used for both surfaces, i.e. $F(\boldsymbol{\sigma}) := F_\mathrm{Y}(\boldsymbol{\sigma}) = F_U(\boldsymbol{\sigma})$. Then, hardening material can be loaded to

$$F(\boldsymbol{\sigma}) \leq \sigma_u. \tag{2}$$

With CT-specimens, the ultimate strength $\sigma_u = R_m$ could be achieved (Staat et al., 2000). In the perfectly plastic theory, $\sigma_u = \sigma_\mathrm{y} = R_{p0.2}$. In safety assessment, only partial use is made of the hardening with $\sigma_u = R_\mathrm{F}$ with the flow stress R_F,

$$R_\mathrm{F} = \frac{R_{p0.2} + R_m}{2}. \tag{3}$$

The structure V is loaded monotonously by the body force $\boldsymbol{q}$ and the surface traction $\boldsymbol{p}$. One may ask for the load factor $\gamma > 1$ by which $\boldsymbol{P} = (\boldsymbol{q}, \boldsymbol{p})$ can be increased up to collapse at $\gamma \boldsymbol{P}$. As long as local plastic flow is limited by surrounding elastic material, no collapse occurs. The limit load theory analyses only the collapse state, in which the structure fails with unrestricted flow without further load increase. Limit load theorems answer the question, when a structure made of ductile material is safe against collapse and when it fails with collapse. For a short and readable presentation of the direct limit load analysis, the reader is referred to Staat and Heitzer (2001).

Static theorem of plastically safe load:

A structure V does not collapse under a load $\gamma \boldsymbol{P}$, if an admissible stress field $\boldsymbol{\sigma}$ can be found, which is in equilibrium with $\gamma \boldsymbol{P}$:

$$\begin{aligned} &F(\boldsymbol{\sigma}) \le \sigma_u \quad \text{in} \quad V, \\ &-\operatorname{div} \boldsymbol{\sigma} = \gamma \boldsymbol{q} \ \text{in} \quad V, \\ &\boldsymbol{\sigma n} = \gamma \boldsymbol{p} \quad \text{on} \quad \partial V_\sigma . \end{aligned} \tag{4}$$

In plasticity a stress is admissible, if it satisfies the yield condition (1) or (2).

For each stress field $\boldsymbol{\sigma}$, which satisfies the conditions of the static theorem, γ is a safety factor, so that the load-carrying capacity of the structure is not yet exhausted. Let us introduce a fictitious elastic stress $\boldsymbol{\sigma}^{\mathrm{E}}$ which is computed for the same loading if the material would be infinitely elastic ($\sigma_{\mathrm{y}} \to \infty$). Then the stress can be decomposed in $\boldsymbol{\sigma}^{\mathrm{E}}$ and a self-equilibrated stress $\boldsymbol{\rho}$, such that $\boldsymbol{\sigma} = \boldsymbol{\sigma}^{\mathrm{E}} + \boldsymbol{\rho}$. One is interested in the largest factor γ, for which the structure does not collapse. One calculates therefore a lower bound of the limit load factor γ_{s} as the largest safety factor from the optimization problem

$$\begin{aligned} &\text{maximize } \gamma, \\ &\text{such that } \quad F(\gamma \boldsymbol{\sigma}^{\mathrm{E}} + \boldsymbol{\rho}) \le \sigma_u \quad \text{in} \quad V, \\ &\qquad\qquad \operatorname{div} \boldsymbol{\rho} = 0 \quad \text{in} \quad V, \\ &\qquad\qquad \boldsymbol{\sigma n} = 0 \quad \text{on} \quad \partial V_\sigma . \end{aligned} \tag{5}$$

There is also a kinematic limit load theorem for the calculation of an upper bound as the smallest overload factor (Staat and Heitzer, 2001). The implementation of the static theorem as a numerical method and its use in the finite element code PERMAS (Intes, 1988) is demonstrated in Staat and Heitzer (2003) and Staat et al. (2000). The extension to the two-surface theory of the kinematic hardening is achieved in Heitzer et al. (2000).

For principle investigations and for the better understanding, closed form limit load solutions are of large practical interest. It is decisive to have reliable limit loads, because over-estimating of burst pressure is clearly non-conservative. But under-estimating of limit loads could also be non-conservative because it leads to under-predicting of CTOD and of crack opening area and consequently also to under-predicting of leak rates.

Limit load theorems are particularly well suited to calculate lower and upper bound solutions of the burst pressure of vessels and piping.

Lower bound analysis by the static theorem:

- Find statically admissible and safe stress fields, for the reference stress which does not exceed the ultimate strength σ_u and which are in equilibrium with the internal pressure.
- Calculate the pressures for each statically admissible stress field. None of them is larger than the true burst pressure.
- Compare the calculated burst pressures. The largest value comes closest to the true burst pressure.

The static theorem under-estimates the collapse pressure. The collapse pressure is overestimated by the upper bound from the kinematic theorem. If however lower and upper bound coincide, then one has found the accurate burst pressure.

A *local* collapse is connected with fully plastic ligament. In that case, the crack will become unstable leading to a penetrating crack. The local collapse may lead to a sudden change in the J-integral curve. The limit load is unique. Therefore, only the *global* collapse load can be computed by limit analysis. It can be identified with gross plastic deformation.

The pipe geometry is characterised through r_1, r_2 and t internal and external radius and wall thickness, respectively. The defect size is characterised by crack depth a and crack length $2c$ as shown in Fig. 1. According to limit analysis, the burst pressure p_{L}

$$p_{\mathrm{L}} = p_{\mathrm{L}}(\sigma_u, a, c, r_1, r_2, t, \ldots), \tag{6}$$

is dimensionally homogeneous of first order in σ_u. Therefore, one may write Eq. (6) in non-dimensional similarity variables

$$\frac{p_{\mathrm{L}}}{\sigma_u} = f(a/t, a/c, t/r_1, r_2/r_1, \ldots). \tag{7}$$

Often the limit load analysis is only understood in a perfectly plastic context. Then, one calls the fictitious load $\gamma_{\mathrm{y}} \boldsymbol{P}$ the limit load and the actual load at failure $\gamma_u \boldsymbol{P}$ the ultimate load (Taylor et al., 1999). For the comparison with experiments, a failure stress σ_u as realistic as possible should be used. In safety assessments conservative material values are used however.

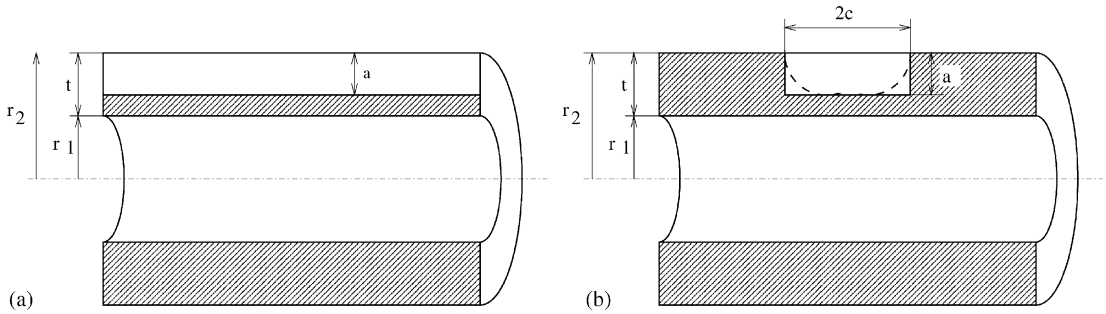

Fig. 1. Through-wall defect and semi-elliptical surface defect in a pipe. (a) Long axial external defect in a pipe. (b) Axial, external surface defect.

It is noticeable that the elastic material constants do not occur in the limit load theorems. However, the stresses in (statically indeterminate structures) depend also on Poisson's ratio ν. Therefore, there is no functional relation between the stresses and the collapse load. Theoretically and experimentally, it has been proven that residual stresses do not have any influence on the limit load, if they do not modify geometry and the yield function.

In the literature (Brocks et al., 1990; Görner and Munz, 1984; Miller, 1988) and in handbooks (Al-Laham, 1999; Andersson et al., 1996; Carter, 1991; Kumar et al., 1981; Schwalbe et al., 1998), different analytic relations were introduced assuming different material behaviour, i.e. different σ_u, and Tresca or von Mises yield function. In order to compare the geometry function $f(a/t, a/c, t/r_1, r_2/r_1, \ldots)$, all references are given in this paper without the authors' specific material assumptions. The different collapse loads can be evaluated more clearly, if one regards first the asymptotic extreme cases defect-free ($a \to 0$), through-wall defect ($a \to t$), very long crack ($c \to \infty$) and short defect ($c \to 0$), thick and thin pipe, and plate (pipe with $r_1 \to \infty$).

2. Thick pipe without defect

2.1. Elastic limit

First yielding starts at the interior wall (radius $r = r_1$) if the internal pressure p_Y is given by

$$\frac{p_Y}{\sigma_y} = D\delta\frac{1-(r_1/r_2)^2}{2} \quad \text{with}$$

$$D = \begin{cases} 1 & \text{for Tresca,} \\ \dfrac{2}{\sqrt{3}} & \text{for von Mises.} \end{cases} \tag{8}$$

For the Tresca hypothesis $\delta = 1$. With the von Mises hypothesis, the boundary conditions at the pipe end must be considered (Szabó, 1972)

$$\delta = \begin{cases} 1 & \text{closed ends,} \\ \left[1+\dfrac{1}{3}\left(\dfrac{r_1}{r_2}\right)^4\right]^{-1/2} & \text{open ends (PS),} \\ \left[1+\dfrac{1}{3}(1-2\nu)^2\left(\dfrac{r_1}{r_2}\right)^4\right]^{-1/2} & \text{plane deformation (PD).} \end{cases} \tag{9}$$

2.2. Plastic collapse

The fully plastic pressure $p_L = p_0$ of the thick-walled pipe without defect is given by

$$\frac{p_0}{\sigma_u} = D\ln\frac{r_2}{r_1} = D\ln\left(1+\frac{t}{r_1}\right)$$

$$= D\left[\frac{t}{r_1} - \frac{1}{2}\left(\frac{t}{r_1}\right)^2 + \frac{1}{3}\left(\frac{t}{r_1}\right)^3 - \frac{1}{4}\left(\frac{t}{r_1}\right)^4 + \cdots\right]. \quad (10)$$

It must be achieved asymptotically by realistic limit load solutions for the cracked pipe. The series expansion converges for $t/r_1 \leq 1$.

The solution for the Tresca hypothesis applies independently of the conditions at the pipe end. For the von Mises hypothesis, the solution does not apply to the open pipe with free ends (Szabó, 1972).

Often for thin pipes, the following approximation is used

$$\frac{\bar{p}_0}{\sigma_u} = D\frac{t}{r_1}. \quad (11)$$

It overrates the load-carrying capacity of thick pipes, as the series expansion (10) shows. For $\nu = 0.3$, the relations remain valid with the Tresca hypothesis up to relatively large thickness ratios

$$\frac{r_2}{r_1} = \begin{cases} 5.43 & \text{closed ends,} \\ 6.19 & \text{open ends,} \\ 5.75 & \text{plain deformation (PD).} \end{cases} \quad (12)$$

The assumption of small deformations does not apply to thicker pipes. The limits in which the relation is valid with the von Mises hypothesis are discussed in Chakrabarty (1987).

In the following, a closed pipe is assumed. It is shown that burst tests in Table 1 are not easily interpreted because of the various uncertainties (Wellinger and Sturm, 1971). It is assumed that form inaccuracies and wall thickness variations of the commercial, seamless pipes used in the experiments contribute substantial uncertainties. Additionally, the first yield could be detected only indirectly on the external wall, without knowledge of the true local wall-thickness (Stoppler, 2000). Table 1 shows that the fully plastic pressure p_0 is a good prediction for burst pressure of a pipe without defects. The dispersions are of comparable magnitude in the linear elastic and in the fully plastic range. First yielding at $p_Y(\sigma_y = R_{p0.2})$ and plastic collapse pressure $p_0(\sigma_u = R_m)$ are apparently lesser overestimated for these burst tests with a Tresca yield surface. Alternatively, one obtains a good estimate for the global collapse if the hardening is only partially considered with the von Mises yield surface and with $p_0(\sigma_u = R_F)$. Therefore, von Mises yield surface and $\sigma_u = R_F$ are assumed from here.

3. Plastic collapse of pipes with penetrating axial cracks

For the collapse load of wall-penetrating longitudinal cracks semi-empirical formulae were set up, which

Table 1
Burst tests (Wellinger and Sturm, 1971), $p_Y(R_{p0.2})$ and $p_0(R_m)$ for the crack-free pipe, $d_2 = 2r_2$

Test	d_2 (mm)	t (mm)	Specimen orientation	$R_{p0.2}$ (MPa)	R_m (MPa)	$p_{Y\,exp}$ (MPa)	p_Y Tresca (MPa)	p_Y von Mises (MPa)	$p_{L\,exp}$ (MPa)	p_L Tresca (MPa)	p_L von Mises (MPa)
AA00	88.9	4.0		336	486	25.5	28.9	33.3	42.7–47.0	45.8	52.9
AB00	88.9	8.8		324	457	58.9	57.8	66.7	94.2–100.6	100.8	116.4
AC00	88.9	22.2		288	438	147.2	107.9	124.6	307.1	303.1	350.0
AK3	101.6	10.0	Longitudinal	284	408				97.5	89.9	103.3
			Transverse	390	457					100.2	115.7
AL1/5	139.7	12.5	Longitudinal	266	400				73.5/76.0	78.9	91.1
			Transverse	338	432					85.2	98.4
CA00	88.9	4.0		512	642	42.2	44.0	50.8	57.9–61.8	60.5	69.93
CB00	88.9	8.8		506	634	87.3	90.3	104.2	135.4–170.7	139.9	161.5
CC00	88.9	22.2		473	614	208.0	177.2	204.7	416.9–421.8	424.9	490.6
HK1/3	101.6	10.0	Longitudinal	689	740				183/175	162.2	187.3
			Transverse	717	759					166.4	192.1
HL1	139.7	12.5	Longitudinal	648	702				152.0	138.4	159.8
			Transverse	668	719					141.8	163.7

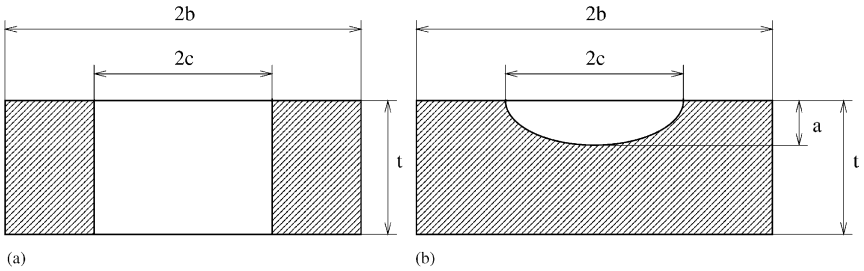

Fig. 2. Penetrating crack and semi-elliptical surface crack in a plate. (a) Penetrating crack in a plate. (b) Semi-elliptical surface crack in a plate.

are often called Battelle formula or slit curve in the literature. According to Hahn et al. (1969) and Kiefner et al. (1973), the burst pressure of the penetrating axial crack is given by ($\sigma_u = R_F$)

$$\frac{\bar{p}_L}{\sigma_u} = D\frac{t}{r_1 M_{FL}}. \tag{13}$$

Here, a Folias factor M_{FL} for longitudinal cracks is used to consider the different behaviour of the plane plate and bulging of the area close to the crack tips in a pipe. This formula is also used in Stoppler et al. (1992, 1994) with $D = 1$ as so-called yield stress criterion. A simple relation for the Folias-factor is

$$M_{FL} = \sqrt{1 + 1.61\frac{c^2}{r_1 t}}. \tag{14}$$

Alternative relations are given in Al-Laham (1999), Görner and Munz (1984), Stoppler et al. (1992, 1994).

For $c \to 0$, all $M_{FL} \to 1$. The burst pressure must then assume the load (10) for the uncracked pipe. Therefore in (13), the often suppressed constraint factor D was already added. Further, the Battelle formula (13) is generalized for thick pipes in Staat (2004) to

$$\frac{p_L}{\sigma_u} = \frac{D}{M_{FL}} \ln\frac{r_2}{r_1}. \tag{15}$$

4. Surface cracks in plates

Limit load solutions for plates with surface cracks (Fig. 2) represent the asymptotic limit for pipes with $r_1 \to \infty$. With surface cracks $c \le b$ in plates, a local collapse (ligament instability) or a global collapse can occur (Al-Laham, 1999; Carter, 1991).

4.1. Local collapse of plates with surface cracks

Ligament instability (local collapse) is caused by the reduced load-carrying section at

$$\frac{\sigma_L}{\sigma_u} = D\left(1 - \frac{a}{t}\right) \tag{16}$$

with the plastic constraint factor D

$$D = \begin{cases} 1 & \text{for plane stress (PS),} \\ \dfrac{2}{\sqrt{3}} & \text{for plane deformation (PD).} \end{cases} \tag{17}$$

σ_L is the nominal stress at plastic collapse referred to a plate of width b and thickness t. Occasionally, more complex expressions with a reduced range of validity were suggested (Görner and Munz, 1984). It is characteristic for the local failure that the load-carrying capacity is exhausted for a penetrating crack with $a \to t$.

4.2. Global collapse of plates with surface cracks

If one sets the bending stress to zero in the relationship of Willoughby and Davey (1989), one obtains a burst pressure σ_L with a global character by

$$\frac{\sigma_L}{\sigma_u} = D\left(1 - \frac{a}{t}\frac{1}{1 + (a/c)/(a/t)}\right). \tag{18}$$

The load-carrying capacity is not exhausted at $a = t$ (and finite crack length c). In Willoughby and Davey (1989), similar solutions are also indicated for embedded cracks.

5. Local collapse of pipes with long surface cracks

5.1. Combination of local plate formulae with thick pipe formulae

In Kumar et al. (1981), a product formula is given, which—in a slightly misleading fracture mechanics view[1]—can be read as local limit load (16) of a plate under the crack-opening hoop stress $\sigma_{\mathrm{L}} = \bar{p}_{\mathrm{L}} r_1/t$ in the thin pipe:

$$\frac{\bar{p}_{\mathrm{L}}}{\sigma_u} = \frac{t}{R_1^*}\frac{\sigma_{\mathrm{L}}}{\sigma_u} = D\frac{t}{R_1^*}\left(1 - \frac{a}{t}\right) \tag{19}$$

with

$$R_1^* = \begin{cases} r_1 & \text{pressure-excluding crack faces,} \\ r_1 + a & \text{pressure-including crack faces.} \end{cases} \tag{20}$$

Eq. (19) is also used in Stoppler et al. (1992, 1994) with $D = 1$ as so-called ligament stress criterion without the distinction of cases (20). Another criterion in Stoppler et al. (1992, 1994), the plastic instability criterion, is similarly structured (a/t is replaced by the ratio of defect area to the load carrying area).

Eq. (19) is the first term in the series expansion for the thick-walled pipe

$$\frac{p_{\mathrm{L}}}{\sigma_u} = D\left(\frac{r_1}{R_1}\right)\ln\left(1 + \frac{t}{r_1}\right)\left(1 - \frac{a}{t}\right), \tag{21}$$

where we propose

$$R_1 = \begin{cases} r_1 & \text{pressure-excluding crack faces,} \\ r_1 + \dfrac{a}{2} & \text{pressure-including crack faces.} \end{cases} \tag{22}$$

An internal pressure load of the crack surfaces reduces the limit load of the pipe in the ratio $r_1/(r_1 + a/2)$. For $a \to 0$, this form tends continuously to the limit of (10). In the pipe and in the plate, plane deformation (PD) with $D = 2/\sqrt{3}$ is assumed here and in the following text.

5.2. Local bounds for long cracks in pipes

The product formulae (19) and (21) with the limiting cases perfect pipe and cracked plate do not correspond to an admissible stress field and have therefore no bounding character according to the limit load theory. One obtains a lower bound for the limit load of a thick pipe with long defect, if one divides the pipe into two coaxial pipes. Pipe 1 carries the defect (pipe with slit on whole length) and is stress free. Pipe 2 is a pipe thinned by a, which carries a homogeneous stress σ_u at collapse.

By this consideration, the collapse load

$$\lim_{c\to\infty}\frac{p_{\mathrm{L}}}{\sigma_u} = D\ln\left(\frac{r_2 - a}{r_1}\right). \tag{23}$$

was obtained in Miller (1988) for the external crack. That is a lower bound solution with a piecewise continuous stress field with $F(\sigma(r)) = \sigma_u$ for $r_1 < r < r_2 - a$. The limit load for the internal defect is wrong in Miller (1988), Carter (1991), Al-Laham (1999). A corrected formula for the internal crack

$$\lim_{c\to\infty}\frac{p_{\mathrm{L}}}{\sigma_u} = D\left[\left(\frac{r_1}{R_1}\right)\left(\frac{r_1 + a}{r_1}\right)\ln\left(\frac{r_2}{r_1 + a}\right)\right] \tag{24}$$

is derived in Staat (2004). R_1 makes the distinction of cases of crack-face loading (22).

6. Collapse of pipes with axial surface defects

6.1. Global collapse

With the global collapse, the longitudinal crack in axial direction becomes unstable and leads in such a way to the vessel bursting. Like before with the plate solutions for long defects, one can generally combine also the global collapse loads of plates with the thick pipe to new limit loads. With the solution (18), one obtains

$$\frac{p_{\mathrm{global}}}{\sigma_u} = D\left(\frac{r_1}{R_1}\right)\ln\left(1 + \frac{t}{r_1}\right) \times \left(1 - \frac{a}{t}\frac{1}{1 + (a/c)/(a/t)}\right). \tag{25}$$

Product formulae from the solutions for the plate and the thick pipe use the case distinction (22) to differentiate the pressure loading condition of the defect faces. However, they do not distinct between internal and external defects. One obtains a lower bound of the global limit load dependent on the defect position, by dividing the pipe into two coaxial pipes, which together are

[1] Limit analysis considers not merely the crack-opening stress but the triaxial stress state, which may lead to plastic flow.

in static equilibrium with the internal pressure (Miller, 1988). Pipe 1 contains the surface crack as penetrating defect. Pipe 2 is intact with a collapse load after (10). Differently than Al-Laham (1999), Miller (1988) and Carter (1991), the slit curve (15) for the thick pipe is used in Staat (2004) to obtain

$$\frac{p_{\text{global}}}{\sigma_u} = D\left[\frac{1}{M_2}\ln\left(\frac{r_2}{r_2-a}\right)+\ln\left(\frac{r_2-a}{r_1}\right)\right] \quad (26)$$

with the shell parameter M_2,

$$M_2 = \sqrt{1+1.61\frac{c^2}{(r_2-a)a}} \quad (27)$$

for the thick pipe with axial surface crack at the external wall. With finite c, Eqs. (25) and (26) achieve the solution (15) of the penetrating defect for $a \to t$. As limit value for $c \to \infty$ one obtains (23), because of $M_2 \to \infty$. A corrected formula for the internal defect

$$\frac{p_{\text{global}}}{\sigma_u} = D\min\left\{\ln\left(\frac{r_2}{r_1}\right);\left(\frac{r_1}{R_1}\right)\left[\frac{1}{M_1}\ln\left(\frac{r_1+a}{r_1}\right)+\left(\frac{r_1+a}{r_1}\right)\ln\left(\frac{r_2}{r_1+a}\right)\right]\right\}. \quad (28)$$

is derived and checked against FEM limit analyses in (Staat, 2004) with the distinction of the pressure loading of the crack faces (22).

6.2. *Local collapse of pipes with axial surface defects*

The defect becomes unstable in wall thickness direction (ligament instability) for fully plastic ligament in the local collapse. Based on experiments with almost rectangular surface cracks in thin pipes and vessels the plate factor after (Kiefner et al., 1973) must be modified with the Folias factor M_{FL}. For the thick pipe, this relationship generalizes to

$$\frac{p_{\text{local}}}{\sigma_u} = D\left(\frac{r_1}{R_1}\right)\ln\left(1+\frac{t}{r_1}\right)\frac{1-(a/t)}{1-(a/M_{\text{FL}}t)}. \quad (29)$$

Occasionally, it is regarded also as a modification of the Battelle formulae (13) or (15) for axial surface cracks (Kastner et al., 1983). From this, a ductility criterion in the sense of the R6 method (Harrison et al., 1980) is derived in Stoppler et al. (1992, 1994) with $R_1 = r_1$, with the approximation (11) for thin pipes and with $D = 1$. For $c \to \infty$ Eq. (14). Then, (29) approaches the solution (21) for the long defect. Eq. (29) does not differentiate according to the defect position, but only according to the load situation of the defect surfaces.

For the thick pipe with external semi-elliptical surface, crack in longitudinal direction (Carter, 1991) gives local collapse loads. With the above modifications, it is shown in Staat (2004) that a better formula is presented by

$$\frac{p_{\text{local}}}{\sigma_u} = \frac{D}{s_2+c}\left[s_2\ln\left(\frac{r_2}{r_1}\right)+c\ln\left(\frac{r_2-a}{r_1}\right)\right] \quad (30)$$

with

$$s_2 = \frac{c\ln(r_2/(r_2-a))(1-(a/t))}{M_2[\ln(r_2/r_1)-\ln((r_2-a)/r_1)] - \ln(r_2/(r_2-a))}. \quad (31)$$

As limit value for $c \to \infty$, one finds (23). A corrected formula for the internal defect is derived in (Staat, 2004) with the distinction of the pressure loading of the crack faces (22).

7. Comparison with burst tests

The database (Stoppler et al., 1992, 1994) burst test nos. 1–134 in Table A.1 in Appendix A could be doubled by new sources. In Germany alone, more than 300 burst-tests with vessels and pipes up to a thickness ratio of $r_2/r_1 = 2$ have been published. Table 2 shows the large parameter range covered by the collected 293 burst tests. For crack-free pipes with $r_2/r_1 = 1.5, \ldots, 5$, additional experiments are found in Uebing (1959). Some experiments could not be assessed, because they were only published with incomplete data. Preliminary tests with different temperatures, notch shapes and sharp fatigue cracks showed that with all surface defects failure could be assumed by fully-plastic collapse, because the notch shape had no influence on the failure pressure (Wellinger and Sturm, 1971; Schulze et al., 1980).[2] Therefore, the experiments were usually carried out with machined notches for simplicity. Characteristic fracture mechanics values

[2] Different to these observations, the experimental burst pressure of pipes with machined slits is reported to have withstood twice the burst pressure of pipes with sharp fatigue cracks (Fuhlrott and Schulze, 1990; Bodmann and Fuhlrott, 1981).

Table 2
Range of data base of 293 burst tests in Table A.1

	$R_{p0.2}$ (MPa)	R_m (MPa)	Y/T ratio ($R_{p0.2}/R_m$)	T (°C)	A_v (J)	r_2	r_2/r_1	a/t	a/c
min	155	416	0.364	−70	6	30	1.02	0.0	0.002
max	1451	1611	0.956	370	261	711	2	1	1

were not generally available. Table A.1 in Appendix A collects 293 experiments with axial defects which are indicated as fatigue cracks only in few cases. The extensive database Kiefner et al. (1973) for thin-walled pipes was not consulted.

The limit load formulae proposed in Section 6 for burst pressures of pipes and vessels with longitudinal defects have the following improvements in relation to the thin pipe formulae, which were available in an earlier evaluation (Stoppler et al., 1992, 1994):

- Only local collapse loads such as (13) have been considered in Stoppler et al. (1992, 1994). Obviously, very deep defects and particularly penetrating cracks (slits) indicate a residual load-carrying capacity, which is better described by the global collapse load.
- The new solutions for thick pipes are safer. The burst pressure is overrated by the thin pipe approximation by approximately 44% for, e.g. $r_2/r_1 = 2$. The dispersions could be reduced, because pipes are assessed with the same accuracy for all values of the thickness ratio.
- Some new formulae consider the crack position (I = internal, E = external) and the pressure loading of the crack faces. This can be used only conditionally, because a specification of the defect location is not always given in the reports on the burst tests. The pressure loading of surfaces of the internal defect is not specified for the tests.
- Without reservation, the new formulae apply to all defect sizes: long, short, shallow (without defect, N) and deep (including penetrating defects, P). Thus, more experiments from a larger parameter range could flow into the comparison. All data from Stoppler et al. (1992, 1994) have been completed, carefully checked and corrected with reference to the original publications.

The failure mode has been given only for some cases in the referred original publications. If crack lengths after test are given, the failure is classified in Table A.1 as break if the length has increased during the test.

The global formula (25) does not consider defect position and can be compared with all burst tests in Figs. 3 and 4. The local formula (25) is represented in Fig. 3 for a thick pipe with $r_1 = t = 22.2$ mm and $\sigma_u = R_F$, $R_F = 0.5(R_{p0.2} + R_m)$. All pressure values are normalized to the burst pressure p_0 of the thick pipe without defect. In Fig. 4, it is plotted for a thin pipe with $r_1 = 355.6$ mm and $t = 8.2$ mm. For thin pipes, the global product formula (25) lies above the local product formula. Therefore, it is expected, that it underestimates the burst pressure and that it is not realistic.

The relative prognosis error *eps*,

$$eps = \frac{p_{\text{exp}} - p_{\text{formula}}}{p_{\text{formula}}} \tag{32}$$

is singular with any local formula for long penetrating defects because $eps \to \infty$ for $p_{\text{formula}} \to 0$ and $p_{\text{exp}} > p_{\text{formula}} > 0$ ($eps \to -1$ for $p_{\text{formula}} \to 0$ and $p_{\text{formula}} > p_{\text{exp}} > 0$). A relative error of 100% or $eps = 1$ means that $p_{\text{exp}} = 2 \cdot p_{\text{formula}}$. Fig. 5 shows the relative error of the global product formula (25) with $\sigma_u = R_F$. Bars to negative errors display overestimations of the burst pressure. Under-estimations

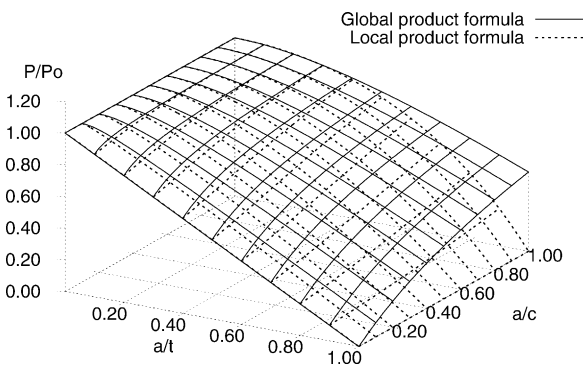

Fig. 3. Product formula p_{local}/p_0 with local formula (29) (for a thick pipe $r_2 = 44.45$ mm, $t = 22.2$ mm) and global formula p_{global}/p_0 (25) with $\sigma_u = R_F$. Global formula —, local formula ···.

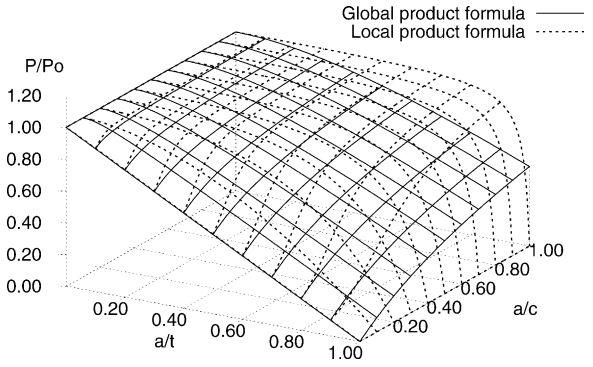

Fig. 4. Product formula p_{local}/p_0 with local formula (29) (for a thin pipe $r_2 = 355.6$ mm, $t = 8.2$ mm) and global formula p_{global}/p_0 (25) to $\sigma_u = R_{\text{F}}$. Global formula —, local formula · · ·.

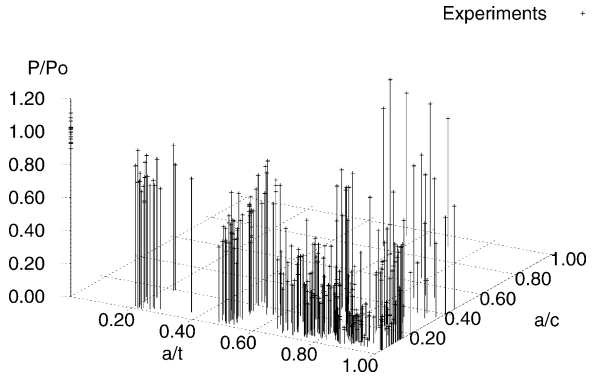

Fig. 6. Burst test with 278 pipes with external defects.

have positive errors. Some larger deviations can be identified as outliers such as, e.g. experiments nos. 60 and 278 which achieve only less than half the burst pressure of comparable tests from the same series, which are already much below the prediction (25). All deep cracks and slits can carry pressures that are more than 100% larger than predicted by the global product formula (25). The residual strength of deep defects suggests that the burst is in fact a global collapse.

The 15 burst tests with internal defects cannot be compared with with formulae (26) and (27) for external defects. Fig. 6 presents the remaining 278 burst tests which can be compared with Figs. 7 and 8 for formulae (26) and (27) for $\sigma_u = R_{\text{F}}$. The global formula (26) predicts larger residual strength of slits than the global product formula (25). Therefore, the scatter of the relative error of the global limit load formula (26) is greatly reduced in Fig. 9, particularly for penetrating defects. FEM analyses in (Staat, 2004) show that Eqs. (26) and (27) slightly over-estimate the burst tests of medium sized short cracks ($a/c \approx 1$). This is also observed in Fig. 9. Other prognosis errors can be attributed to uncertainties of geometry and strength.

The strong penetrating defect is an outlier no. 231 which achieves a two times higher pressure than no. 232. The dispersion of the burst pressure is naturally larger for pipes with large defects than for the perfect pipes without defects. The emphasis of all experiments is with deep defects. This is reason enough to expect a larger span here. However, the relatively large scatter for large defects could be attributed to the growth of the prognosis error *eps* Eq. (32) for $p_{\text{formula}} \to 0$. This ex-

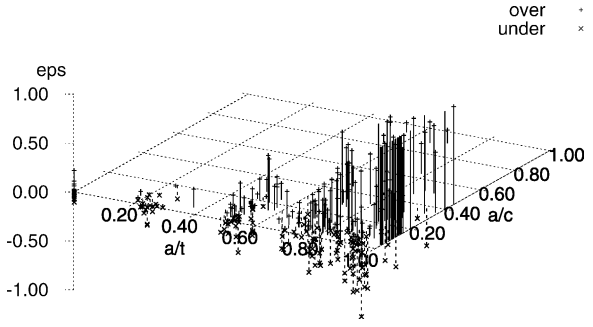

Fig. 5. Relative prognosis error of global product formula (25) with $\sigma_u = R_{\text{F}}$: (— +) burst pressure under-rated, (—) burst pressure under-rated by more than 100%, (· · · ×) burst pressure over-rated.

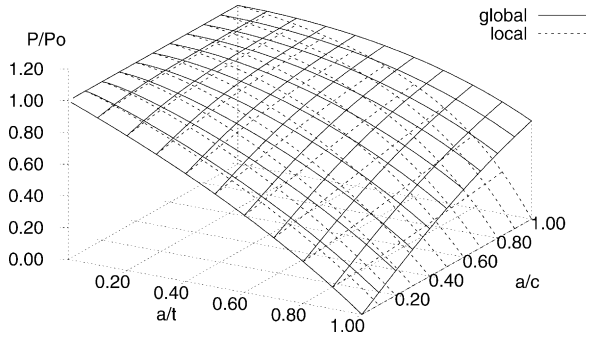

Fig. 7. Global and local collapse load p_{global}/p_0 and p_{local}/p_0 for external cracks in thick pipes and vessels Eq. (26) and Eqs. (30), (31), respectively, with $r_2/r_1 = 2$ and $\sigma_u = R_{\text{F}}$. Global formula —, local formula · · ·.

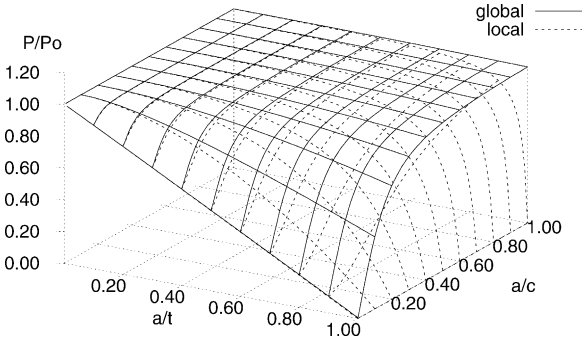

Fig. 8. Global and local collapse load p_{global}/p_0 and p_{local}/p_0 for external cracks in thin pipes and vessels Eq. (26) and Eqs. (30), (31), respectively, with $r_2/r_1 = 1.02$ and $\sigma_u = R_{\text{F}}$. Global formula —, local formula $\cdots$.

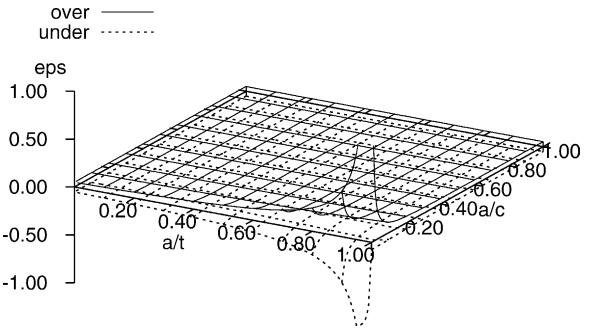

Fig. 10. Relative prognosis error for ±5% variation of wall thickness t in global formula (26) plotted for a thin pipe ($r_2/r_1 = 1.02$): (— +) burst pressure under-rated, ($\cdots \times$) burst pressure over-rated.

plains the apparent increase of the uncertainty for long deep defects. Let the wall thickness t of the pipes vary with ±5% and all other data be exact. Then, the size $t - a$ of the ligament becomes uncertain and the global formula (26) predicts under-ratings and over-ratings as shown in Fig. 10 for a thin pipe. The negative values of the relative error *eps* are small for penetrating defects, because the crack depth a is bounded by t. A similar behaviour is observed for the experimental uncertainty in Fig. 11 which shows that the relative error is rather small for most penetrating defects. Therefore, it can be assumed that the scatter is mainly due to the uncertainty of geometrical and strength data and that burst tests can be explained by global plastic collapse. In this demonstration, the assumption of ±5% variation of t is not justified for welded pipes and vessels. But Table 1 shows that welded pipes may have similarly large strength uncertainities of strength from texture instead. Moreover, the best definition of σ_u may be different for different materials. Therefore, the scatter may be partly caused by the unified assumption $\sigma_u = R_{\text{F}}$ for all tests. Finally, it is observed in Fig. 8 that the global collapse pressure of thin pipes has a steep gradient and is therefore very sensitive to uncertainties of the aspect ratio a/c for deep and long defects ($a/c < 0.2$).

It was the objective of the comparison with experiments to find good estimates for the ultimate strength of flawed pressure vessels and pipes. In order to achieve conservative predictions of the burst pressure, it is important to choose conservative combinations of the geometric and material data. Alternatively, a probabilistic fracture mechanics approach could be employed (Staat, 1995). In connection with the two-criteria method (SINTAP procedure, FAD, R6 method (Harrison et al., 1980; R6, 2001; Ainsworth, 2000)) one obtains more conservative assessments of the axial fatigue cracks by use of a Tresca yield surface (i.e. $D = 1$) and $\sigma_u = R_{\text{F}}$.

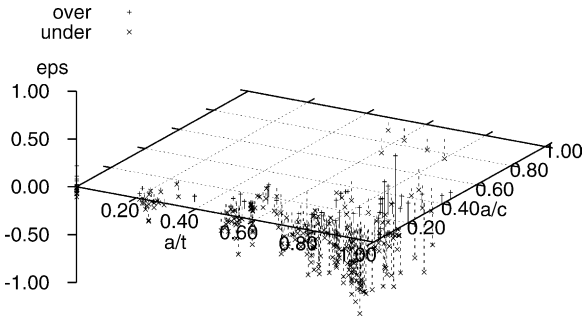

Fig. 9. Relative prognosis error of global formula (26) with $\sigma_u = R_{\text{F}}$: (— +) burst pressure under-rated, ($\cdots \times$) burst pressure over-rated.

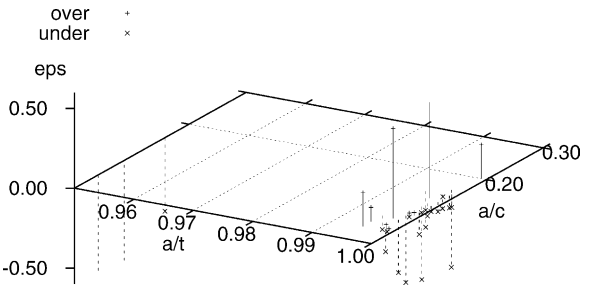

Fig. 11. Relative prognosis error of global formula (26) with $\sigma_u = R_{\text{F}}$ for very deep external cracks and slits: (— +) burst pressure under-rated, ($\cdots \times$) burst pressure over-rated.

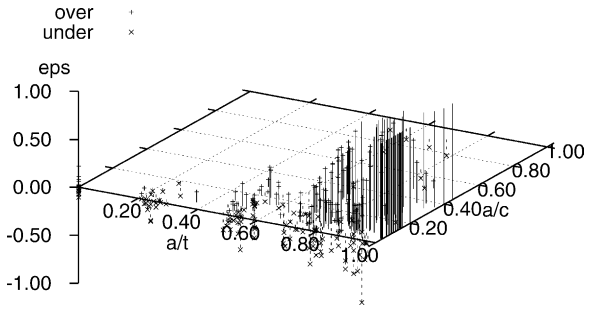

Fig. 12. Relative prognosis error of local formula (30) with (31) with $\sigma_u = R_F$: (— +) burst pressure under-rated, (—) burst pressure under-rated by more than 100%, ($\cdots\times$) burst pressure over-rated.

As is the case for almost all available burst tests this fracture mechanics assessment often fails in practice, because of the missing fracture toughness data, which could only be estimated here, e.g. from the Charpy-V notch impact energy A_v. As a structural mechanics method, limit analysis enables a realistic assessment on the basis of simple strength data.

The experiments concentrate on long defects with $a/c < 0.2$ where the differences between local and global burst pressure are small. This is also the case for shallow defects. Few more experiments with deep short defects with $a/t > 0.8$ and $0.3 < a/c < 1$ would be helpful. Fig. 12 shows that the local collapse formula (30) with (31) has lesser over-ratings than an global formula. But a local formula does not represent the residual load-carrying capacity of deep cracks. Burst pressure of deep defects with, e.g. $a/t = 0.9$ is under-rated by more than 200% and *eps* is singular for penetrating cracks.

Comparing Figs. 3, 4 with Figs. 7, 8 suggests that the local product formula (29) may serve as a simple alternative to the local formula (30) with (31). The global product formula (25) cannot be recommended.

8. Conclusions

In earlier investigations, local formulae for collapse loads of crack containing pipes indicated large uncertainties, even if their range of validity has been restricted. Local formulae have infinitely large error for slits. They do not represent the residual load carrying capacity of pipes with deep cracks.

New local and global collapse loads for thick-walled pipes have been proposed in product form and in form of an additive combination of limiting cases. They are compared with a large number of burst tests in a wide range of pipe and defect dimensions for different materials. It could be shown that the additive global collapse loads for axial defects can predict burst pressures of pipes or pressure vessels for all dimensions of defects including slits. Limit load solutions have the advantage that in practice all material data are available.

Due to uncertain geometrical and material data, the uncertainty of collapse pressure predictions increases for long and deep cracks. More conservative assessment may be achieved if fracture mechanics data is given additionally. Then, the two-criteria method could be used to combine the fracture dominated and the collapse dominated failure mechanisms for predictions of burst pressures.

Acknowledgement

J. Hoffmann helped to solve problems with LaTeX 2_ε and gnuplot.

Appendix A

See Table A.1.

Table A.1
Data basis of burst tests

No.	Test	Leak/ break	Defect position	p_{exp} (MPa)	Geometry data				Characteristic dim.			Material data			
					r_2 (mm)	t (mm)	a (mm)	c (mm)	r_2/r_1	a/t	a/c	Material/reference	$R_{p0.2}$ (MPa)	R_m (MPa)	A_v (J)
1	AA3I	B	I	39.0	44.45	4.0	0.8	39.5	1.10	0.20	0.02	St 35 (Wellinger and Sturm, 1971)	336	486	76
2	AA3H	B	I	34.1	44.45	4.0	2	22.5	1.10	0.50	0.08		336	486	
3	AA4A	(B)	I	26.7	44.45	4.0	2	46.5	1.10	0.50	0.04		336	486	
4	AA3F	L	I	23	44.45	4.0	2	122.5	1.10	0.50	0.02		336	486	
5	AA3D	L	I	19.1	44.45	4.0	2.6	51	1.10	0.65	0.06		336	486	
6	AA3B	B	E	33.4	44.45	4.0	1.1	33	1.10	0.28	0.04		336	486	
7	AA8A	L	E	34.3	44.45	4.0	1	58	1.10	0.25	0.02		336	486	
8	AA4F	B	E	36	44.45	4.0	2	10	1.10	0.50	0.20		336	486	
9	AA4I	L	E	33.6	44.45	4.0	2.3	13.5	1.10	0.58	0.18		336	486	
10	AA3E	B	E	27.5	44.45	4.0	2	36	1.10	0.50	0.06		336	486	
11	AA8E	L	E	27.5	44.45	4.0	2	61	1.10	0.50	0.04		336	486	
12	AA3G	L	E	22.4	44.45	4.0	2	111	1.10	0.50	0.02		336	486	
13	AA8D	B	E	21.2	44.45	4.0	2.1	110	1.10	0.53	0.02		336	486	
14	AA3C	L	E	17.9	44.45	4.0	2.8	37.5	1.10	0.70	0.08		336	486	
15	AA8C	L	E	14.7	44.45	4.0	3	62.5	1.10	0.75	0.04		336	486	
16	AA6A	L	E	8.34	44.45	4.0	3.1	42.5	1.10	0.78	0.08		336	486	
17	AA6G	L	E	16.0	44.45	4.0	3.6	20	1.10	0.90	0.18		336	486	
18	AA6F	L	E	26.5	44.45	4.0	3.6	15	1.10	0.90	0.24		336	486	
19	AB14A	B	E	63.8	44.45	8.8	4.6	64.5	1.25	0.52	0.08		324	457	33
20	AB2D	L	E	51.0	44.45	8.8	4.6	116	1.25	0.52	0.04		324	457	
21	AB2F	L	E	49.5	44.45	8.8	4.5	266	1.25	0.51	0.02		324	457	
22	AB2M	L	E	71.1	44.45	8.8	6.3	18.5	1.25	0.72	0.34		324	457	
23	AB2L	L	E	48.1	44.45	8.8	6.3	43.5	1.25	0.72	0.14		324	457	
24	AB14B	B	E	42.7	44.45	8.8	6.1	67	1.25	0.69	0.10		324	457	
25	AB2I	L	E	35.3	44.45	8.8	6.3	118.5	1.25	0.72	0.06		324	457	
26	AB14E	B	E	31.4	44.45	8.8	6.2	120	1.25	0.70	0.06		324	457	
27	AB2N	L	E	30.4	44.45	8.8	6.3	268.5	1.25	0.72	0.02		324	457	
28	AB14D	B	E	28.3	44.45	8.8	6.7	270	1.25	0.76	0.02		324	457	
29	AB6A	L	E	58.9	44.45	8.8	8	25	1.25	0.91	0.32		324	457	
30	AB6B	L	E	57.9	44.45	8.8	8.5	25	1.25	0.97	0.34		324	457	
31	AB7D	B	I	80.2	44.45	8.8	1.8	46.5	1.25	0.20	0.04		324	457	
32	AB7C	B	I	71.8	44.45	8.8	4	32	1.25	0.45	0.12		324	457	
33	AB7K	B	I	61.6	44.45	8.8	4.2	57.5	1.25	0.48	0.08		324	457	
34	AB6E	(B)	I	56.7	44.45	8.8	4.3	133	1.25	0.49	0.04		324	457	
35	AB7I	B	I	47.1	44.45	8.8	6.1	64	1.25	0.69	0.10		324	457	
36	AB2K	B	E	88.8	44.45	8.8	2	10.5	1.25	0.23	0.20		324	457	
37	AB2H	B	E	77.5	44.45	8.8	1.94	35.5	1.25	0.22	0.06		324	457	
38	AB14C	B	E	77.5	44.45	8.8	2.2	61	1.25	0.25	0.04		324	457	
39	AB1M	B	E	77.0	44.45	8.8	1.9	110.5	1.25	0.22	0.02		324	457	
40	AB1L	(B)	E	77.0	44.45	8.8	1.9	260.5	1.25	0.22	0.00		324	457	
41	AB2E	B	E	72.1	44.45	8.8	4.5	16	1.25	0.51	0.28		324	457	
42	AB1K	B	E	60.8	44.45	8.8	4.6	41	1.25	0.52	0.12		324	457	
43	AB8	L	E	48.0	44.45	8.8	8.2	30	1.25	0.93	0.28		324	457	
44	AB6M	L	E	49.1	44.45	8.8	8.1	32.5	1.25	0.92	0.24		324	457	
45	AB6C	L	E	15.7	44.45	8.8	8.2	100	1.25	0.93	0.08		324	457	
46	AC6A	B	I	274.7	44.45	22.2	4	57	2.00	0.18	0.08		288	438	56
47	AC5E	B	I	209.9	44.45	22.2	10.8	51	2.00	0.49	0.22		288	438	
48	AC6D	B	I	184.4	44.45	22.2	11.4	77	2.00	0.51	0.14		288	438	
49	AC6E	B	I	164.3	44.45	22.2	11.2	151.5	2.00	0.50	0.08	St 35 (Wellinger and Sturm, 1971)	288	438	56
50	AC5D	B	I	136.2	44.45	22.2	15.7	85.5	2.00	0.71	0.18		288	438	
51	AC7A	B	E	260	44.45	22.2	4.2	40.5	2.00	0.19	0.10		288	438	
52	AC5B	B	E	254.1	44.45	22.2	4.8	41.5	2.00	0.22	0.12		288	438	
53	AC11A	B	E	255.1	44.45	22.2	4.5	64.5	2.00	0.20	0.06		288	438	
54	AC7C	B	E	201.1	44.45	22.2	11.2	49	2.00	0.50	0.22		288	438	
55	AC11B	B	E	184.4	44.45	22.2	11.2	80.5	2.00	0.50	0.14		288	438	
56	AC7B	B	E	161.4	44.45	22.2	10.1	122.5	2.00	0.45	0.08		288	438	

Table A.1 (*Continued*)

No.	Test	Leak/ break	Defect position	p_{exp} (MPa)	Geometry data				Characteristic dim.			Material data			
					r_2 (mm)	t (mm)	a (mm)	c (mm)	r_2/r_1	a/t	a/c	Material/reference	$R_{p0.2}$ (MPa)	R_m (MPa)	A_v (J)
57	AC7E	B	E	167.8	44.45	22.2	15.9	52	2.00	0.72	0.30		288	438	
58	AC11C	B	E	147.2	44.45	22.2	15.5	85.5	2.00	0.70	0.18		288	438	
59	AK3C	L		39.5	50.8	10.0	9	35	1.25	0.90	0.26	St 35 (Sturm and Stoppler, 1985)	337	433	80
60	AK2G	L		2.3	50.8	10.0	9.3	230	1.25	0.93	0.04		337	433	
61	AK3F	L		13.3	50.8	10.0	8.6	90	1.25	0.86	0.10		337	433	
62	AK3D	L		27.0	50.8	10.0	8.5	60	1.25	0.85	0.14		337	433	
63	AK3E	L		37.4	50.8	10.0	9	40	1.25	0.90	0.22		337	433	
64	AK2B	L		5.0	50.8	10.0	9.4	230	1.25	0.94	0.04		337	433	
65	AK3E	B		56.0	50.8	10.0	7.5	35	1.25	0.75	0.22		337	433	
66	AK2B	B		25.5	50.8	10.0	8.2	230	1.25	0.82	0.04		337	433	
67	AK2G	B		10.5	50.8	10.0	9	230	1.25	0.90	0.04		337	433	
68	AK3F	B		28.3	50.8	10.0	8	100	1.25	0.80	0.08		337	433	
69	AK3D	B		26.0	50.8	10.0	8	90	1.25	0.80	0.08		337	433	
70	AL5C	B		8.0	69.85	12.5	11	350	1.22	0.88	0.04		302	416	
71	AL5D	L		21.2	69.85	12.5	10	70	1.22	0.80	0.14		302	416	
72	AL5E	L		6.4	69.85	12.5	11	140	1.22	0.88	0.08		302	416	
73	AL1C	L		26	69.85	12.5	11.1	50	1.22	0.89	0.22		302	416	
74	AL1C	L		31.0	69.85	12.5	8.8	50	1.22	0.70	0.18		302	416	
75	KWU1	L	E	19.7	162.3	22.3	19	150	1.16	0.85	0.12	20 MnMoNi 5 5 (Kastner et al., 1983)	449	608	
76	KWU2	L	E	15.0	162.2	22.24	18.7	378.85	1.16	0.84	0.04		449	608	
77	KWU3	L	E	18.8	162.35	22.54	17.9	378.4	1.16	0.79	0.04		449	608	
78	KWU4	B	E	22.5	162.35	22.57	17.5	378.2	1.16	0.78	0.04		449	608	
79	KWU5	B	E	22.25	162.3	22.32	17.25	378.2	1.16	0.77	0.04		449	608	
80	GWF01	L	E	2.6	355.6	8.2	7.8	102.5	1.02	0.95	0.08	St 70 (Geilenkeuser and Sturm, 1976)	543	695	50
81	GWF02	L	E	2.8	355.6	8.2	7.5	105	1.02	0.91	0.08		543	695	
82	GWF03	L	E	4.6	355.6	8.2	7.14	100	1.02	0.87	0.08		543	695	
83	GWF04	B	E	6.0	355.6	8.2	6.2	125	1.02	0.76	0.04		543	695	
84	GWF05	L	E	6.2	457.2	10.6	9.2	100	1.02	0.87	0.10		529	670	115
85	GWF06	B	E	6.4	457.2	10.6	7.2	125	1.02	0.68	0.06		529	670	
86	BMI04			17.2	304.8	43.3	33	360.7	1.17	0.76	0.10	A 106 B (Eibner et al., 1971)	235	562	92
87	BMI08			15.9	304.8	43.7	32.3	311.15	1.17	0.74	0.10		218	509	81
88	BMI09			9.38	304.8	41.9	36.8	311.15	1.16	0.88	0.12		241	570	
89	BMI18			11.17	304.8	17.8	9	136.55	1.06	0.51	0.06		240	553	68
90	BMI19			29.65	304.8	41.1	26.7	147.3	1.16	0.65	0.18		232	568	88
91	BMI20			13.51	304.8	17.3	8.9	66.7	1.06	0.51	0.14		259	544	68
92	BMI24			22.2	304.8	38.1	22.9	147.3	1.14	0.60	0.16	Type 316 (Eibner et al., 1971)	159	431	200
93	BMI25			27.93	304.8	38.1	22.9	76.2	1.14	0.60	0.30		155	426	
94	BMI26			24.68	304.8	38.1	17.8	147.3	1.14	0.47	0.12	A 316 (Eibner et al., 1971)	155	426	200
95	BMI27			16.55	95.25	9.7	6.2	71.75	1.11	0.64	0.08	A 106 B (Eibner et al., 1971)	201	500	61
96	BMI28			18.82	95.25	12.7	9.4	111.15	1.15	0.74	0.08		209	570	
97	BMI32			11.31	95.25	12.1	10.3	254	1.15	0.85	0.04		248	583	
98	HL1C	B	E	12	69.85	12.5	11	350	1.22	0.88	0.04	11 NiMnCrMo 5 5 (Sturm and Stoppler, 1985)	658	711	80
99	HL1D2	L	E	48	69.85	12.5	10	70	1.22	0.80	0.14		658	711	
100	HL1	L	E	36.7	69.85	12.5	10.4	82.5	1.22	0.83	0.12		658	711	
101	HL2	L	E	37.5	69.85	12.5	10.7	90	1.22	0.86	0.12		658	711	
102	HL3	L	E	32.2	69.85	12.5	10.7	120	1.22	0.86	0.08		658	711	
103	HL4	L	E	24	69.85	12.5	11.6	125	1.22	0.93	0.10		658	711	
104	HL5	L	E	21.5	69.85	12.5	11.2	160	1.22	0.90	0.08		658	711	
105	HL6	L	E	19.0	69.85	12.5	11.4	190	1.22	0.91	0.06		658	711	
106	HL7	B	E	17.5	69.85	12.5	11.3	225	1.22	0.90	0.06		658	711	
107	HL8	B	E	33.0	69.85	12.5	10.4	140	1.22	0.83	0.08		658	711	
108	HL1E1	L	E	16.0	69.85	12.5	11	140	1.22	0.88	0.08		658	711	
109	BVZ022	L	E	21.9	398.95	47.2	38.2	391	1.13	0.81	0.10	20 MnMoNi 5 5 (Sturm and Stoppler, 1985)	415	601	214

Table A.1 (*Continued*)

No.	Test	Leak/ break	Defect position	p_{exp} (MPa)	Geometry data				Characteristic dim.			Material data			
					r_2 (mm)	t (mm)	a (mm)	c (mm)	r_2/r_1	a/t	a/c	Material/reference	$R_{p0.2}$ (MPa)	R_m (MPa)	A_v (J)
110	BVZ030	B	E	19.5	398.95	47.2	36.2	750	1.13	0.77	0.04		426	612	
111	BVZ060	(B)	E	18.0	398.95	47.2	36	750	1.13	0.76	0.04		423	624	
112	BVZ070	L	I	22.4	398.95	47.2	38.2	350	1.13	0.81	0.10		427	605	
113	BVZ080	L	E	20.4	398.95	47.2	36.2	750	1.13	0.77	0.04		513	636	
114	BVS020	(B)	E	14.8	396.95	47.2	37.3	354.5	1.13	0.79	0.10	22 NiMoCr 37 special heat (Sturm and Stoppler, 1985)	383	622	42
115	BVS042	B	E	16.8	396.95	47.2	38.3	354.5	1.13	0.81	0.10		410	613	62
116	BVS030	B	E	13.1	396.95	47.2	35	550	1.13	0.74	0.06		366	601	42
117	HK1D	B	E	52.0	50.8	10.0	7.5	250	1.25	0.75	0.04	11 NiMnCrMo 5 5 (Sturm and Stoppler, 1985)	703	750	40
118	HK1F	B	E	48.3	50.8	10.0	8	100	1.25	0.80	0.08		703	750	
119	HK1F	L	E	97.5	50.8	10.0	9	35	1.25	0.90	0.26		703	750	
120	HK1G	L	E	26	50.8	10.0	9.5	60	1.25	0.95	0.16		703	750	
121	HK1G	L	E	32	50.8	10.0	9	75	1.25	0.90	0.12		703	750	
122	HK1F	L	E	82.5	50.8	10.0	9	40	1.25	0.90	0.22		703	750	
123	HK1G	B	E	31.5	50.8	10.0	9	90	1.25	0.90	0.10		703	750	
124	HK6C	B	E	41.0	50.8	10.0	8.2	100	1.25	0.82	0.08		703	750	
125	HK1G	L	E	74.5	50.8	10.0	8.5	48	1.25	0.85	0.18		703	750	
126	HK1G	B	E	64.5	50.8	10.0	8.5	60	1.25	0.85	0.14		703	750	
127	HK2A	B	E	53.0	50.8	10.0	8	185	1.25	0.80	0.04		703	750	
128	HK2B	B	E	31.5	50.8	10.0	8.5	185	1.25	0.85	0.04		703	750	
129	HK2C	B	E	25.0	50.8	10.0	9	185	1.25	0.90	0.04		703	750	
130	HK2D	L	E	7.7	50.8	10.0	9.5	230	1.25	0.95	0.04		703	750	
131	HK2D	B	E	24.0	50.8	10.0	9.3	230	1.25	0.93	0.04		703	750	
132	HK2G	L	E	10.7	50.8	10.0	9.4	230	1.25	0.94	0.04		703	750	
133	HK6D	B	E	123.0	50.8	10.0	2.6	100	1.25	0.26	0.02		703	750	
134	HK6E	B	E	87.0	50.8	10.0	5	100	1.25	0.50	0.06		703	750	
135	AA00		N	42.7	44.45	4.0	0.0	0	1.10	0.00	–	St 35 (Wellinger and Sturm, 1971)	336	486	76
136	AA00		N	47.0	44.45	4.0	0.0	0	1.10	0.00	–		336	486	
137	AB00		N	94.18	44.45	8.8	0.0	0	1.25	0.00	–		324	457	33
138	AB00		N	100.6	44.45	8.8	0.0	0	1.25	0.00	–		324	457	
139	AC00		N	307.1	44.45	22.2	0.0	0	2.00	0.00	–		288	438	56
140	AC13K	B	E	229.6	44.45	22.2	4.6	76	2.00	0.21	0.06		288	438	56
141	AC13L	L	E	233.5	44.45	22.2	4.6	76	2.00	0.21	0.06		235	549	
142	AC13H	B	E	229.6	44.45	22.2	4.6	76	2.00	0.21	0.06		235	549	
143	AC12C	B	E	178.5	44.45	22.2	11.2	74	2.00	0.50	0.16		288	438	
144	AC12D	B	E	180.5	44.45	22.2	11.2	74	2.00	0.50	0.16		288	438	
145	AC12E	B	E	180.5	44.45	22.2	11.2	74	2.00	0.50	0.16		288	438	
146	AC12I	B	E	184.4	44.45	22.2	11.2	74	2.00	0.50	0.16		288	438	
147	AC12H	B	E	178.5	44.45	22.2	11.2	74	2.00	0.50	0.16		288	438	
148	AC12F	L	E	168.7	44.45	22.2	11.2	74	2.00	0.50	0.16		235	549	
149	AC12G	B	E	172.7	44.45	22.2	11.2	74	2.00	0.50	0.16		235	549	
150	AC12B	B	E	164.8	44.45	22.2	11.2	74	2.00	0.50	0.16		199	471	
151	AC13E	L	E	108.9	44.45	22.2	19.7	83	2.00	0.89	0.24		288	438	
152	AC13D	L	E	99.8	44.45	22.2	19.7	83	2.00	0.89	0.24		288	438	
153	AC13A	L	E	113.8	44.45	22.2	19.7	83	2.00	0.89	0.24		288	438	
154	AC13B	L	E	114.8	44.45	22.2	19.7	83	2.00	0.89	0.24		288	438	
155	CA00		N	57.9	44.45	4.0	0.0	0	1.10	0.00	–	FB 70 (Wellinger and Sturm, 1971)	512	642	44
156	CA00		N	61.8	44.45	4.0	0.0	0	1.10	0.00	–		512	642	
157	CA1E	B		31.4	44.45	4.0	2.0	36	1.10	0.50	0.06		512	642	
158	CA1D	L		26.5	44.45	4.0	2.0	111	1.10	0.50	0.02		512	642	
159	CB00		N	135.4	44.45	8.8	0.0	0	1.25	0.00	–		506	634	42
160	CB00		N	170.7	44.45	8.8	0.0	0	1.25	0.00	–		506	634	
161	CB2B	B	E	105.9	44.45	8.8	2.0	10	1.25	0.23	0.20		506	634	
162	CB2C	B	E	100.1	44.45	8.8	2.0	35	1.25	0.23	0.06		506	634	
163	CB4D	L	E	103.0	44.45	8.8	2.0	110	1.25	0.23	0.02		506	634	
164	CB2E	L	E	99.1	44.45	8.8	2.0	260	1.25	0.23	0.01		506	634	
165	CB6D	B	E	109.9	44.45	8.8	4.2	15	1.25	0.48	0.28		506	634	
166	CB6A	B	E	78.5	44.45	8.8	4.2	40	1.25	0.48	0.10		506	634	
167	CB6B	L	E	66.7	44.45	8.8	4.2	115	1.25	0.48	0.04		506	634	
168	CB6C	L	E	63.8	44.45	8.8	4.2	265	1.25	0.48	0.02		506	634	
169	CB6E	B	E	98.8	44.45	8.8	6.0	18	1.25	0.68	0.34		506	634	

Table A.1 (*Continued*)

No.	Test	Leak/ break	Defect position	p_{exp} (MPa)	Geometry data				Characteristic dim.			Material data			
					r_2 (mm)	t (mm)	a (mm)	c (mm)	r_2/r_1	a/t	a/c	Material/reference	$R_{p0.2}$ (MPa)	R_m (MPa)	A_v (J)
170	CB6F	B	E	55.9	44.45	8.8	6.0	43	1.25	0.68	0.14		506	634	
171	CB1B	B	E	41.2	44.45	8.8	6.0	118	1.25	0.68	0.06		506	634	
172	CB4E	L	E	37.3	44.45	8.8	6.0	268	1.25	0.68	0.02		506	634	
173	CB8B	B	E	29.2	44.45	8.8	6.7	269	1.25	0.76	0.02		506	634	
174	CC00		N	416.9	44.45	22.2	0.0	0	2.00	0.00	–		473	614	71
175	CC00		N	421.8	44.45	22.2	0.0	0	2.00	0.00	–		473	614	
176	CC1B	B	E	255.1	44.45	22.2	11	48	2.00	0.50	0.22		473	614	
177	CC1A	B	E	219.7	44.45	22.2	11	123	2.00	0.50	0.08		473	614	
178	HK1		N	183.0	50.8	10.0	0.0	0	1.25	0.00	–	11 NiMnCrMo 5 5 (Sturm and Stoppler, 1985)	703	750	40
179	HK3		N	175.0	50.8	10.0	0.0	0	1.25	0.00	–		703	750	
180	HL1		N	152.0	69.85	12.5	0.0	0	1.22	0.00	–		658	711	80
181	AK3		N	97.5	50.8	10.0	0.0	0	1.25	0.00	–	St 35 (Sturm and Stoppler, 1985)	337	433	80
182	AL1		N	73.5	69.85	12.5	0.0	0	1.22	0.00	–		302	416	
183	AL5		N	76.0	69.85	12.5	0.0	0	1.22	0.00	–		302	416	
184	AB2M	L		71.1	44.45	8.8	6.25	18.5	1.25	0.71	0.34		324	457	80
185	AB2L	L		48.1	44.45	8.8	6.27	43.5	1.25	0.71	0.14		324	457	
186	AB2I	L		35.3	44.45	8.8	6.28	117.5	1.25	0.71	0.05		324	457	
187	AB2M	(B)	P	62.8	44.45	8.8	(8.6)	19.5	1.25	1.00	0.45		324	457	
188	AB2M	B	P	58.9	44.45	8.8	(8.6)	22	1.25	1.00	0.40		324	457	
189	AB2L	B	P	37.3	44.45	8.8	(8.7)	43.5	1.25	1.00	0.20		324	457	
190	AB2I	B	P	12.8	44.45	8.8	(8.7)	95	1.25	1.00	0.09		324	457	
191	BVZ010	L	P	23.8	398.75	47.6	(47.6)	325	1.14	1.00	0.15	20 MnMoNi 55 (Sturm and Stoppler, 1985)	520	633	200
192	BVZ011	L	P	14.8	399.15	47.6	(47.6)	551	1.14	1.00	0.09		515	632	
193	BVZ012	L	P	14.4	399.15	47.6	(47.6)	552.5	1.14	1.00	0.09		515	632	
194	BVS010		P	17.5	395.95	47.4	(47.6)	400	1.14	1.00	0.12	22 NiMoCr 37 mod (1985)	480	603	50
195	GWF4		P	3.26	355.6	8.2	(8.2)	206.85	1.02	1.00	0.04	St 70 (Geilenkeuser and Sturm, 1976)	543	695	50
196	GWF5		P	3.0	355.6	8.2	(8.2)	222.35	1.02	1.00	0.03		543	695	
197	GWF6		P	3.0	355.6	8.2	(8.2)	234.35	1.02	1.00	0.03		543	695	
198	GWF7		P	2.47	355.6	8.2	(8.2)	238.8	1.02	1.00	0.03		543	695	
199	GWF12		P	9.09	355.6	8.2	(8.2)	54.7	1.02	1.00	0.15		543	695	
200	GWF13		P	9.0	355.6	8.2	(8.2)	56.05	1.02	1.00	0.13		543	695	
201	GWF14		P	8.68	355.6	8.2	(8.2)	61.1	1.02	1.00	0.13		543	695	
202	GWF15		P	8.26	355.6	8.2	(8.2)	65.25	1.02	1.00	0.12		543	695	
203	GWF16		P	7.89	355.6	8.2	(8.2)	72.05	1.02	1.00	0.11		543	695	
204	GWF17		P	7.6	355.6	8.2	(8.2)	78.7	1.02	1.00	0.10		543	695	
205	GWF18		P	7.19	355.6	8.2	(8.2)	84.3	1.02	1.00	0.09		543	695	
206	GWF19		P	6.53	355.6	8.2	(8.2)	97.8	1.02	1.00	0.08		543	695	
207	AC12A	B	E	184.4	44.45	22.2	11.2	74	2.00	0.50	0.15	St 35 cooled ($-75\,^{\circ}$C to $-60\,^{\circ}$C) (Wellinger and Sturm, 1971)	304	500	6
208	AC13F	B	E	115.8	44.45	22.2	19.7	83	2.00	0.88	0.23		304	500	
209	AC13C	B	E	91.2	44.45	22.2	19.7	83	2.00	0.88	0.23		304	500	
210	BC4E	B	E	186.4	44.45	22.2	11.2	74	2.00	0.50	0.15	St 35 unkilled (Wellinger and Sturm, 1971)	280	419	12
211	BC4G	B	E	182.5	44.45	22.2	11.2	74	2.00	0.50	0.15		280	419	
212	BC4H	B	E	185.9	44.45	22.2	11.2	74	2.00	0.50	0.15		280	419	
213	BC4I	B	E	183.4	44.45	22.2	11.2	74	2.00	0.50	0.15		280	419	
214	HD1A	L	E	22.0	282.0	18.4	16.8	109	1.07	0.91	0.15	34CrMo4 at 20 $^{\circ}$C fatigue crack (Keller, 1990)	798	922	78
215	HD2B	B	E	43.0	282.5	18.0	9.3	72	1.07	0.52	0.22		778	925	59
216	HD3	B	E	31.7	283.0	18.0	11.6	107.5	1.07	0.64	0.11		703	847	80
217	HD4	L	E	33.4	283.0	17.8	15.8	75	1.07	0.89	0.21		751	886	79
218	HD5	B	E	50.0	282.5	20.4	16.1	48	1.08	0.79	0.34		878	990	64
219	HD6	B	E	55.5	283.0	21.7	14.5	32.5	1.08	0.67	0.45		866	979	65
220	HD8	B	E	48.7	282.5	17.6	15.0	31.5	1.07	0.85	0.48		813	944	59
221	HD16	B	E	28.2	285.5	17.7	13.1	80	1.07	0.74	0.16		831	947	68
222	HD17	B	E	29.0	282.5	17.6	11.6	102.5	1.07	0.66	0.28		832	966	68

Table A.1 (*Continued*)

No.	Test	Leak/ break	Defect position	p_{exp} (MPa)	Geometry data				Characteristic dim.			Material data			
					r_2 (mm)	t (mm)	a (mm)	c (mm)	r_2/r_1	a/t	a/c	Material/reference	$R_{p0.2}$ (MPa)	R_m (MPa)	A_v (J)
223	HD9	B	E	46.2	282.5	17.5	13.0	47	1.07	0.74	0.27	34CrMo4 at −20 °C fatigue crack (Keller, 1990)	859	982	77
224	HD10	B	E	40.8	282.5	18.4	14.7	77.5	1.07	0.80	0.19		853	973	75
225	HD11	B	E	44.7	283.5	18.5	10.7	71.5	1.07	0.58	0.15		842	985	63
226	HD12	B	E	37.3	282.5	17.7	9.0	107.5	1.07	0.51	0.08		830	984	65
227	HD13	B	E	49.0	283.0	17.8	10.0	71	1.07	0.56	0.14		726	879	81
228	HD14	B	E	56.4	282.5	18.7	13.5	46.5	1.07	0.72	0.29		843	976	76
229	HD15	L	E	28.5	282.0	18.0	17.8	49	1.07	0.99	0.36	34CrMo4 at −20 °C (Keller, 1990)	825	966	65
230	1	B		38.0	38.2	3.2	1.7	8.5	1.09	0.53	0.20	15Mo3 at 20 °C (Fuhlrott and Schulze, 1990)	335	490	166
231	2	B	P	25.2	38.3	3.3	(3.3)	25	1.09	1.00	0.13		335	490	
232	3	B	P	12.2	38.4	3.4	(3.4)	50	1.10	1.00	0.07		335	490	
233	5	L		35.3	38.8	3.8	3.2	8.5	1.11	0.84	0.38		335	490	
234	6	L		19.6	38.2	3.2	2.4	22.5	1.09	0.75	0.11		335	490	
235	7	L		15.3	38.4	3.4	2.8	32.5	1.10	0.82	0.09		335	490	
236	8	L		17.3	38.4	3.4	2.6	57.5	1.10	0.76	0.05		335	490	
237	13	L		26.1	39.0	4.0	3.1	22.5	1.11	0.78	0.14		335	490	
238	14	L		20.7	38.9	3.9	3.1	32.5	1.11	0.79	0.10		335	490	
239	15	L		15.7	38.9	3.9	3.1	57.5	1.11	0.79	0.05		335	490	
240	16	L		26.0	39.0	4.0	3.1	22.5	1.11	0.78	0.14		335	490	
241	17	L		18.9	39.0	4.0	3.4	32.5	1.11	0.85	0.10		335	490	
242	18	L		17.5	39.0	4.0	3.4	57.5	1.11	0.85	0.06		335	490	
243	9	L		15.7	38.4	3.4	2.3	57.5	1.10	0.68	0.04	15Mo3 at 20 °C with torsion 3kNm (Fuhlrott and Schulze, 1990)	335	490	
244	10	L		19.4	38.4	3.4	2.6	32.5	1.10	0.76	0.08		335	490	
245	11	L		20.3	38.8	3.8	3.1	32.5	1.11	0.82	0.10		335	490	
246	12	L		23.6	39.0	4.0	3.1	32.5	1.11	0.78	0.10		335	490	
247	19	L		16.3	38.8	3.8	3.0	40	1.11	0.79	0.08	15Mo3 at 200 °C (Fuhlrott and Schulze, 1990)	305	454	168
248	20	L		14.1	38.9	3.9	2.9	62.5	1.11	0.74	0.05		305	454	
249	F1	B	P	10.4	44.45	4.0	(4.0)	25.0	1.10	1.00	0.16	15Mo3 at 370 °C (Bodmann and Fuhlrott, 1981; Fuhlrott and Schulze, 1990)	246	570	84
250	F2	B	P	7.7	44.45	4.0	(4.0)	37.0	1.10	1.00	0.11		246	570	
251	F3	B	P	6.2	44.45	4.0	(4.0)	50.0	1.10	1.00	0.08		246	570	
252	F4	B	P	6.0	44.45	4.0	(4.0)	60.0	1.10	1.00	0.07		246	570	
253	F5	L	E	16.3	44.45	4.0	3.7	10.0	1.10	0.93	0.37		246	570	
254	F6	L	E	10.7	44.45	4.0	3.8	10.0	1.10	0.95	0.38		246	570	
255	F7	L	E	7.6	44.45	4.0	3.7	15.0	1.10	0.93	0.25		246	570	
256	F8	B	E	14.2	44.45	4.0	3.3	20.0	1.10	0.83	0.17		246	570	
257	F9	L	E	8.0	44.45	4.0	3.7	20.0	1.10	0.93	0.19		246	570	
258	F10	L	E	7.8	44.45	4.0	3.5	25.0	1.10	0.88	0.14		246	570	
259	F11	B	E	14.5	44.45	4.0	3.2	30.0	1.10	0.80	0.11		246	570	
260	F12	L	E	6.2	44.45	4.0	3.6	30.0	1.10	0.90	0.12		246	570	
261	F13	L	E	7.3	44.45	4.0	3.5	40.0	1.10	0.88	0.09		246	570	
262	F14	L	E	9.2	44.45	4.0	3.5	40.0	1.10	0.88	0.09		246	570	
263	F15	L	E	11.7	44.45	4.0	3.1	45.0	1.10	0.78	0.07		246	570	
264	A1	B	P	13.1	30.15	2.0	(2.0)	13.6	1.05	1.00	0.15	X10 CrNiTi 18 9 fatigue crack (Bodmann and Fuhlrott, 1981; Fuhlrott and Schulze, 1990)	316	641	
265	A2	B	P	8.35	30.15	2.0	(2.0)	28.3	1.05	1.00	0.07		316	641	
266	A3	B	P	7.25	30.15	2.0	(2.0)	39.8	1.05	1.00	0.05		316	641	
267	A4	B	P	5.95	30.15	2.0	(2.0)	54.8	1.05	1.00	0.04		316	641	
268	A5	B	E	6.8	30.15	2.0	1.8	31.8	1.05	0.90	0.06	X10 CrNiTi 18 9 (Bodmann and Fuhlrott, 1981; Fuhlrott and Schulze, 1990)	316	641	
269	A6	B	E	7.0	30.15	2.0	1.72	51.8	1.05	0.86	0.04		316	641	
270	A7	L	E	6.7	30.15	2.0	1.81	26.8	1.05	0.90	0.07		316	641	

Table A.1 (*Continued*)

No.	Test	Leak/ break	Defect position	p_{exp} (MPa)	Geometry data				Characteristic dim.			Material data			
					r_2 (mm)	t (mm)	a (mm)	c (mm)	r_2/r_1	a/t	a/c	Material/reference	$R_{p0.2}$ (MPa)	R_m (MPa)	A_v (J)
271	A8	B	E	6.5	30.15	2.0	1.74	71.8	1.05	0.87	0.03		316	641	
272	A9	L	E	6.7	30.15	2.0	1.82	21.8	1.05	0.91	0.09		316	641	
273	A10	B	E	7.0	30.15	2.0	1.77	31.8	1.05	0.89	0.06		316	641	
274	A11	L	E	5.5	30.15	2.0	1.83	26.8	1.05	0.92	0.07		316	641	
275	A12	B	E	6.5	30.15	2.0	1.8	31.8	1.05	0.90	0.06		316	641	
276	A13	B	E	8.4	30.15	2.0	1.8	26.8	1.05	0.90	0.07		316	641	
277	A14	L	E	4.7	30.15	2.0	1.83	26.8	1.05	0.92	0.07		316	641	
278	A15	L	E	3.2	30.15	2.0	1.8	26.8	1.05	0.90	0.07		316	641	
279	A16	L	E	6.6	30.15	2.0	1.79	21.8	1.05	0.90	0.09		316	641	
280	A17	B	E	7.3	30.15	2.0	1.74	71.8	1.05	0.87	0.03		316	641	
281	A18	L	E	5.1	30.15	2.0	1.8	40.0	1.05	0.90	0.05		316	641	
282	ESAT1	B	E	48.3	212.0	8.0	5.7	6.25	1.04	0.71	0.91	48 CrMoNiV 4 10 (D6AC) fatigue crack, K_{IC} = 140 MPa$\sqrt{m}$ (Agatonovic, 1997, 2000)	1450.7	1611.1	
283	ESAT2	B	E	56.3	212.0	8.0	3.95	4.11	1.04	0.49	0.96		1450.7	1611.1	
284	ESAT3	B	E	53.6	212.0	8.0	4.5	4.8	1.04	0.56	0.94		1450.7	1611.1	
285	ESAT6	B	E	13.8	144.0	6.0	3.3	4.0	1.04	0.55	0.83	Al 2219 T62 fatigue crack, K_{IC} = 60 MPa$\sqrt{m}$ (Agatonovic, 1997, 2000)	266.1	388	
286	ESAT7	B	E	12.3	144.0	6.0	4.7	7.35	1.04	0.78	0.64		266.1	388	
287	ESAT8	B	E	14.3	144.0	6.0	4.0	4.5	1.04	0.67	0.89		266.1	388	
288	ESAT9	B	E	6.08	141.0	3.0	2.6	5.05	1.02	0.79	0.51		266.1	388	
289	ESAT10	B	E	6.0	141.0	3.0	2.7	5.3	1.02	0.90	0.51		266.1	388	
290	846077	B		15.35	711.2	19.25	10.4	90.0	1.03	0.54	0.12	API X100 triggered by explosion (Mannucci et al., 2001)	740	774	261
291	846014	B		20.12	711.2	20.1	3.8	192.5	1.03	0.19	0.002		795	840	171
292	99457	B		21.4	457.2	16.4	9.0	75.0	1.04	0.55	0.12		739	813	253
293	99457	B		24.02	457.2	16.4	6.0	225.0	1.04	0.37	0.03		739	813	253

Defect positions: I, internal; E, external; N: none; P, penetrating.

References

Agatonovic, P., 1997. Development of residual strength evaluation tool based on stress-strain approximation. Int. J. Fracture 88, 129–152.

Agatonovic, P., 2000. Private communication.

Al-Laham, S., 1999. Stress Intensity Factor and Limit Load Handbook. British Energy Report EPD/GEN/REP/0316/98, Issue 2.

Andersson, P., Bergman, M., Brickstad, B., Dahlberg, L., Nilsson, F., Sattari-Far, I., 1996. A Procedure for Safety Assessment of Components With Cracks—Handbook. SAQ/FoU-Report 96/08, SAQ Kontrol AB, Stockholm.

Ainsworth, R.A., 2000. Foreword: Special issue on flaw assessment methods. Int. J. Pressure Vessels Piping 77, 853.

Bodmann, E., Fuhlrott, H., 1981. Investigation of Critical Crack Geometries in Pipes. SMiRT 6, Paris, paper L6/6.

Brocks, W., Fuhlrott, H., Keller, H.P., Munz, D., Schulze, H.-D., 1990. Bruchmechanik druckbeanspruchter Bauteile. Hanser, München und TÜV Rheinland, Köln.

Carter, A.J., 1991. A Library of Limit Loads for FRACTURE.TWO. Nuclear Electric, Internal Report TD/SID/REP/0191.

Chakrabarty, J., 1987. Theory of Plasticity. McGraw-Hill, New York.

Fuhlrott, H., Schulze, H.-D., 1990. Längs- und Umfangsfehler in Rohren und Behältern unter Innendruck und äußeren Belastungen. In Brocks et al. (1990).

Geilenkeuser, H., Sturm, D., 1976. Rißausbreitung in Großrohren aus dem Stahl St 70. gwf-gas/erdgas 117, 40–43.

Görner, F., Munz, D., 1984. Plastische Instabilität. In: Munz, D. (Ed.), Leck-vor-Bruch-Verhalten druckbeaufschlagter Komponenten. Fortschr. Ber. VDI-Z. Reihe, 18, Nr. 14, VDI-Verlag, Düsseldorf.

Hahn, G.T., Sarrate, M., Rosenfield, A.R., 1969. Criteria for crack extension in cylindrical pressure vessels. Int. J. Fracture Mech. 5, 187–210.

Harrison, R.P., Loosemore, K., Milne, I., Dowling, A.R., 1980. Assessment of the integrity of structures containing defects. CEGB Report R/H/R6-Rev. 2.

Heitzer, M., Pop, G., Staat, M., 2000. Basis reduction for the shakedown problem for bounded kinematic hardening material. J. Global Optim. 17, 185–200.

Intes, 1988. PERMAS User's Reference Manuals. Stuttgart, Intes Publication Nos. 202, 207, 208, 302, UM 404, UM 405.

Kastner, W., Lochner, H., Rippel, R., Bartholomé, G., Keim, E., Gerscha, A., 1983. Untersuchung zur instabilen Rißausbreitung und zum Rißstoppverhalten. Kraftwerk Union Report R 914/83/018, Erlangen.

Keller, H.P., 1990. Leistungsvergleich von Methoden der Rißerfassung und -bewertung am Beispiel von axialen Oberflächenrissen in Behältern unter Innendruck. In Brocks et al. (1990).

Kiefner, J.F., Maxey, W.A., Eiber, R.J., Duffy, A.R., 1973. Failure Stress Loads of Flaws in Pressurized Cylinders. ASTM STP 536, Philadelphia, pp. 461–481.

Kumar, V., German, M.D., Shih, C.F., 1981. An Engineering Approach for Elastic–Plastic Fracture Analysis. EPRI NP-1931, New York.

Miller, A.G., 1988. Review of limit loads of structures containing defects. Int. J. Pressure Vessels Piping 32, 197–327.

Mannucci, G., Demofonti, G., Harris, D., Barsanti, L., Hillenbrand, H.-G., 2001. Fracture Properties of API X100 Gas Pipeline Steels. EP-TP39–01en, Europipe, Ratingen, Germany.

R6, 2001. Assessment of the integrity of structures containing defects. British Energy, Rev. 4.

R5, 2003. An assessment procedure for the high temperature response of structures. British Energy, Rev. 3.

Schulze, H.D., Togler, G., Bodmann, E., 1980. Fracture mechanics analysis on the initiation and propagation of circumferential and longitudinal cracks in straight pipes and pipe bends. Nucl. Eng. Des. 58, 19–31.

Schwalbe, K.-H., Zerbst, U., Kim, Y.-J., Brocks, W., Cornec, A., Heerens, J., Amstutz, H., 1998. EFAM ETM 97—the ETM method for assessing the significance of crack-like defects in engineering structures, comprising the versions ETM 97/1 and ETM 97/2. Report GKSS 98/E/6, Geesthacht.

Staat, M., 1995. Reliability of an HTR-Module Primary Circuit Pressure Boundary: Influences, Sensitivity, and Comparison with a PWR. Nucl. Eng. Des. 158, 333–340.

Staat, M., Heitzer, M., Yan, A.M., Khoi, V.D., Nguyen, D.H., Voldoire, F., Lahousse, A., 2000. Limit Analysis of Defects. Berichte des Forschungszentrums Jülich, Jül-3746.

Staat, M., Heitzer, M., 2001. LISA - a European Project for FEM-based Limit and Shakedown Analysis. Nucl. Eng. Des. 206, 151–166.

Staat, M., Heitzer, M. (Eds.), 2003. Numerical Methods for Limit and Shakedown Analysis. NIC-Series, vol. 15. John von Neumann Institute for Computing, Jülich, http://www.fz-juelich.de/nic-series/volume15/nic-series-band15.pdf.

Staat, M., 2004. Local and global collapse of longitudinally flawed pipes and cylindrical vessels. Int. J. Pressure Vessels Piping, in press.

Stoppler, W., Shen, S.M., de Boer, A., 1992. Versagensanalyse von längsfehlerbehafteten Rohren und Behältern. 22. Technischer Bericht, BMU-1992–347.

Stoppler, W., Sturm, D., Scott, P., Wilkowski, G., 1994. Analysis of the failure behaviour of longitudinally flawed pipes and vessels. Nucl. Eng. Des. 151, 425–448.

Stoppler, W., 2000. Private communication.

Sturm, D., Stoppler, W., 1985. Forschungsvorhaben Phänomenologische Behälterberstversuche—Traglast- und Berstverhalten von Rohren mit Längsfehlern. Förderkennzeichen 150 279, Phase 1, Forschungsbericht MPA Stuttgart.

Szabó, I., 1972. Höhere Technische Mechanik. Springer, Berlin.

Taylor, N., et al., 1999. The Design-by-Analysis Manual. Report EUR 19020 EN, European Commission, DG-JRC/IAM, Petten (1999).

Uebing, D., 1959. Festigkeitsverhalten dickwandiger Hohlzylinder unter Innendruck im vollplastischen Bereich. Thesis, TH Stuttgart.

Wellinger, K., Sturm, D., 1971. Festigkeitsverhalten von zylindrischen Hohlkörpern. Fortschr. Ber. VDI-Z. Reihe 5, Nr. 13, VDI-Verlag, Düsseldorf.

Willoughby, A.A., Davey, T.G., 1989. Plastic Collapse in Part-Wall Flaws in Plates. ASTM STP 1020, Philadelphia, pp. 390–409.